Pietrobon, D. (1986) *Bioelectrochem. Bioenerg. 15*, 193–209.
Pietrobon, D., & Caplan, S. R. (1985) *FEBS Lett. 192*, 119–122.
Pietrobon, D., Zoratti, M., Azzone, G. F., Stucki, J. W., & Walz, D. (1982) *Eur. J. Biochem. 127*, 483–494.
Rottenberg, H. (1978) *FEBS Lett. 94*, 295–297.
Rottenberg, H., Caplan, S. R., & Essig, A. (1967) *Nature (London) 216*, 610–616.
Slater, E. C., Berden, J. A., & Herweijer, M. A. (1985) *Biochim. Biophys. Acta 811*, 217–231.
Stoner, C. D. (1985) *J. Bioenerg. Biomembr. 17*, 85–108.
van Dam, K., Westerhoff, H. V., Krab, K., van der Meer, R., & Arents, J. C. (1980) *Biochim. Biophys. Acta 591*, 240–250.
van der Bend, R. L., & Herweijer, M. A. (1985) *FEBS Lett. 186*, 8–10.
Venturoli, G., & Melandri, B. A. (1982) *Biochim. Biophys. Acta 680*, 8–16.
Westerhoff, H. V. (1983) Ph.D. Thesis, University of Amsterdam, Amsterdam, The Netherlands.
Westerhoff, H. V., Colen, A. M., & van Dam, K. (1983) *Biochem. Soc. Trans. 11*, 81–85.
Westerhoff, H. V., Melandri, B. A., Venturoli, G., Azzone, G. F., & Kell, D. B. (1984) *Biochim. Biophys. Acta 768*, 257–292.
Williams, R. J. P. (1961) *J. Theor. Biol. 1*, 1–17.
Zoratti, M., Pietrobon, D., & Azzone, G. F. (1982) *Eur. J. Biochem. 126*, 443–451.

Double-Inhibitor and Uncoupler–Inhibitor Titrations. 2. Analysis with a Nonlinear Model of Chemiosmotic Energy Coupling

Daniela Pietrobon*,‡,§ and S. Roy Caplan‡

Department of Membrane Research, The Weizmann Institute of Science, Rehovot 76100, Israel, and CNR Unit for the Study of the Physiology of Mitochondria and Institute of General Pathology, University of Padova, 35100 Padova, Italy

Received December 11, 1985; Revised Manuscript Received July 15, 1986

ABSTRACT: The results of double-inhibitor and uncoupler–inhibitor titrations have been simulated and analyzed with a nonlinear model of delocalized protonic coupling obtained by linking two proton pump models of the kind studied by Pietrobon and Caplan [Pietrobon, D., & Caplan, S. R. (1985) *Biochemistry 24*, 5764–5776] through their common intermediate $\Delta\tilde{\mu}_H$. It is shown that the results predicted by a delocalized chemiosmotic model are highly dependent on the kind of relationships existing between rate of ATP synthesis, J_p, and $\Delta\tilde{\mu}_H$ and rate of electron transfer, J_e, and $\Delta\tilde{\mu}_H$. With nonlinear flow–force relationships all the results reported so far are not necessarily inconsistent with the delocalized chemiosmotic model provided that the relationships between rates and $\Delta\tilde{\mu}_H$ satisfy the following requirements: $\partial J_p/\partial\Delta\tilde{\mu}_H$ increases and/or $\partial J_e/\partial\Delta\tilde{\mu}_H$ decreases as $|\Delta\tilde{\mu}_H|$ increases.

In the preceding paper we analyzed the results of double-inhibitor and uncoupler–inhibitor titrations obtained for a delocalized chemiosmotic model of energy coupling (Mitchell, 1966) with linear flow–force relationships (between the rate of electron transfer and $\Delta\tilde{\mu}_H$,[1] and between the rate of ATP synthesis and $\Delta\tilde{\mu}_H$). However, the flow–force relationships measured in many energy-transducing systems (see references below) and also those simulated on the basis of simple kinetic models of ion pumps (Hansen et al., 1981; Chapman et al., 1983; Lauger, 1984; Pietrobon & Caplan, 1985) are approximately linear only in limited ranges of $\Delta\tilde{\mu}_H$. The measured relation between rate of electron transfer and $\Delta\tilde{\mu}_H$ obtained by decreasing $|\Delta\tilde{\mu}_H|$ below its static head value is characterized by a region of approximate linearity extending over 40–50 mV and by a saturation region of maximum electron flow at lower $|\Delta\tilde{\mu}_H|$ (Padan & Rottenberg, 1973; Nicholls, 1974; Azzone et al., 1978a; van Dam et al., 1980; Pietrobon et al., 1982). The measured relation between rate of ATP synthesis and $\Delta\tilde{\mu}_H$ is usually characterized by a threshold value of $|\Delta\tilde{\mu}_H|$ below which no ATP synthesis occurs and above which there is a sharp nonlinear dependence of the rate of ATP synthesis on $\Delta\tilde{\mu}_H$ (see for example the relations obtained by inhibiting the rate of electron transfer in mitochondria, e.g., Zoratti et al., 1982; Mandolino et al., 1983; Yagi et al., 1984; or those obtained by decreasing the light intensity in photophosphorylating systems, e.g., Graber & Witt, 1976; Baccarini Melandri et al., 1977; Hangarter & Good, 1982; Clark et al., 1983; or those obtained by varying an artificially imposed $\Delta\tilde{\mu}_H$, e.g., Graber, 1982). The general flow–force relationships for the six-state proton pump model studied by Pietrobon and Caplan (1985) are sigmoidal, a common characteristic of models of ion pumps or cotransport systems involving cyclic reaction schemes with only one voltage-dependent step (Hansen et al., 1981; Chapman et al., 1983).

The conclusion of the preceding paper that the published results of double-inhibitor titrations are inconsistent with a

‡ The Weizmann Institute of Science.
§ University of Padova.

[1] Abbreviations: $\Delta\tilde{\mu}_H$, transmembrane difference in the electrochemical potential of protons; $\Delta\psi$, transmembrane difference of electrical potential; ATPase, adenosinetriphosphatase; ATP, adenosine triphosphate; A_e, affinity of the electron-transfer reaction; A_p, affinity of the ATP hydrolysis reaction; n_p, stoichiometry H^+/ATP of the ATPase pump; n_e, stoichiometry H^+/e^- of the redox pump; J_e, rate of electron transfer; J_p, rate of ATP synthesis or hydrolysis ($J_p > 0$, hydrolysis; $J_p < 0$, synthesis); f_e, inhibition factor of the redox pumps; f_p, inhibition factor of the ATPases.

0006-2960/86/0425-7690$01.50/0

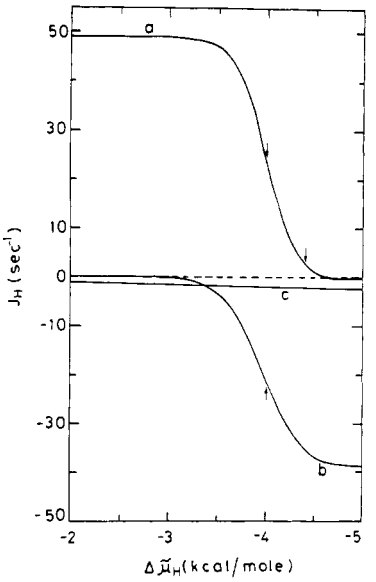

FIGURE 1: Relationships between the proton flow, J_H, and $\Delta\tilde{\mu}_H$: (a) redox pump; (b) ATPase pump; (c) leak. Simulations performed with the proton pump model described in Pietrobon and Caplan (1985) with the kinetic parameters of pump B and affinity A_e = 19.66 kcal/mol to simulate the proton efflux through a redox pump (curve a), and with the kinetic parameters of pump A and affinity A_p = 6 kcal/mol to simulate the proton influx through an ATPase pump (curve b). L_H^l = 0.5 mol kcal^{-1} (curve c). The matched arrows on curves a and b indicate the phosphorylating stationary state of zero net proton flow (state 3). The arrow at higher $\Delta\tilde{\mu}_H$ indicates the stationary state of zero net proton flow (static head) in the presence of excess ATPase inhibitor.

delocalized chemiosmotic model (in the presence of a negligible leak) was reached with linear flow–force relationships and cannot be extended to the case of nonlinear relationships. This was pointed out earlier by Westerhoff and co-workers (Westerhoff et al., 1983; Westerhoff, 1983) and recently demonstrated by Davenport (1985).

In this paper the results of double-inhibitor and uncoupler–inhibitor titrations are simulated and analyzed with a nonlinear chemiosmotic model obtained by linking two proton pump models of the kind studied by Pietrobon and Caplan (1985) through their common intermediate $\Delta\tilde{\mu}_H$. With the help of the linear analysis presented in the accompanying paper, this modeling study allows one to establish what kind of nonlinear flow–force relations can give rise to results different from those obtained in the linear case. It is shown that none of the results of double-inhibitor and uncoupler–inhibitor titrations reported so far in the literature are inconsistent with the delocalized chemiosmotic model of energy coupling provided that the relationships between rates and $\Delta\tilde{\mu}_H$ satisfy certain requirements. These requirements are illustrated and discussed in relation to the relevant experiments.

Analysis of Double-Inhibitor Titrations

In a previous paper (Pietrobon & Caplan, 1985) we determined and studied the general flow–force relations for a six-state proton pump model with and without intrinsic uncoupling. The model can be used as a simplified representation of either a reversible ATPase proton pump [pump A in Pietrobon and Caplan (1985)] or of an irreversible redox proton pump [pump B in Pietrobon and Caplan (1985)], by choosing the appropriate equilibrium constant and set of rate constants in the simulation. Figure 1 shows the simulated dependence on $\Delta\tilde{\mu}_H$ of the proton flow through the $\Delta\tilde{\mu}_H$ generating redox pump (positive efflux in our sign convention, curve a) and of the proton flow through the $\Delta\tilde{\mu}_H$ utilizing ATPase pump (negative influx, curve b). In simulation a the affinity of the redox reaction is kept constant at a high value to simulate the experimental situation in which an excess of redox substrate is present, while in simulation b the affinity of the ATP hydrolysis reaction is kept constant at a low value to simulate the experimental situation in which ADP is added to start phosphorylation. Also shown in Figure 1 is the dependence on $\Delta\tilde{\mu}_H$ of the third element of the chemiosmotic protonic circuit, the proton leak, which is assumed here to be Ohmic (curve c). $\Delta\tilde{\mu}_H$ is varied by varying $\Delta\psi$ with ΔpH = 0, so that in these simulations $\Delta\tilde{\mu}_H = \Delta\psi$. As the driving force $|\Delta\tilde{\mu}_H|$ decreases, the proton influx through the ATPase decreases from its maximum value in the saturation region at high $|\Delta\tilde{\mu}_H|$ and approaches zero at values of $|\Delta\tilde{\mu}_H|$ higher than the equilibrium value ($\Delta\tilde{\mu}_H^{eq} = -A_p/n_p$ since the pump is assumed to be completely coupled). Below this value no proton efflux coupled to ATP hydrolysis occurs. At the low value of the affinity of the ATP hydrolysis reaction used the kinetically reversible ATPase pump behaves as if it were kinetically irreversible (Pietrobon & Caplan, 1985). The experimental relationships measured in different systems between proton influx though the ATPase and $\Delta\tilde{\mu}_H$ are very similar to the simulation given by curve b in Figure 1 (Graber, 1982; Maloney & Hansen, 1982; Clark et al., 1983; Zoratti et al., 1986). It is worthwhile noting that for the following discussion of double-inhibitor titrations it does not matter whether this kind of relationship reflects the dependence of the enzyme turnover on $\Delta\tilde{\mu}_H$ (as in the model) or the dependence on $\Delta\tilde{\mu}_H$ of the number of active ATPases, each of which translocates protons at its maximum rate [as is probably the case in broken chloroplasts in the absence of reducing agents (Graber et al., 1984; Mills & Mitchell, 1984; Rumberg & Becker, 1984)].

If the proton pumps are assumed to be fully coupled the rate of electron transfer is given at any $\Delta\tilde{\mu}_H$ by the proton efflux (curve a) divided by n_e, while that of ATP synthesis is given by the rate of proton influx (curve b) divided by n_p. In Figure 1 and in the following considerations a small intrinsic uncoupling (which accounts for the results of static head experiments in mitochondria (Pietrobon et al., 1981; Pietrobon et al., 1986) is actually allowed in the redox pump so that J_e is slightly higher than J_H/n_e (curve a) (Pietrobon & Caplan, 1985). To facilitate discussion and since intrinsic uncoupling does not qualitatively affect the results of double-inhibitor titrations, the ATPase pump is assumed to be fully coupled.

The arrow on curve a at high $|\Delta\tilde{\mu}_H|$ indicates the stationary state of zero net proton flow (static head) attained by the chemiosmotic system when the ATPases are completely inhibited and the only possible influx of protons is through the leak. In the absence of ATPase inhibitor, under phosphorylating conditions, the total proton influx at any $\Delta\tilde{\mu}_H$ is given by the sum of the influxes through the ATPases and through the leak (curves b and c), and the chemiosmotic system reaches a different stationary state of zero net proton flow (state 3) at lower $|\Delta\tilde{\mu}_H|$, indicated by the matched arrows on curves a and b. A given pair of reaction affinities A_e and A_p defines a unique state 3. With the rate constants used in the simulations of Figure 1 state 3 falls slightly above the inflection point, in the middle of the region of approximate linearity of the flow force curve for the ATPase pump.

Figure 2 (continuous lines) shows the rate of ATP synthesis, J_p (plotted in a conventional way), as a function of $\Delta\tilde{\mu}_H$ (as would be obtained experimentally by decreasing $|\Delta\tilde{\mu}_H|$ with uncouplers or redox inhibitors below its state 3 value) in the absence of ATPase inhibitor (f_p = 1) or in the presence of concentrations of inhibitor that decrease the number of AT-

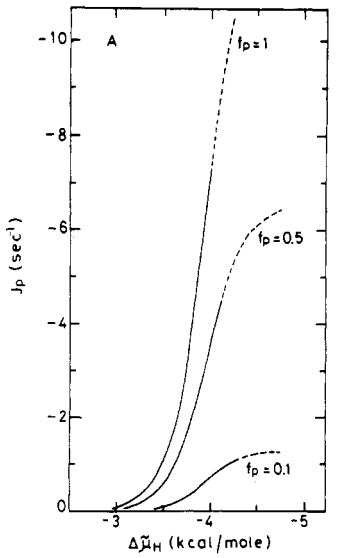

FIGURE 2: Continuous lines: rate of ATP synthesis, J_p, as a function of $\Delta\tilde{\mu}_H$, as would be obtained by decreasing $\Delta\tilde{\mu}_H$ below the state 3 value with uncouplers or redox inhibitors, for f_p = 1, 0.5, and 0.1. Dashed lines: dependence of J_p on $\Delta\tilde{\mu}_H$ at $|\Delta\tilde{\mu}_H|$ higher than the state 3 values. Parameters of the simulations as in Figure 1 (case A).

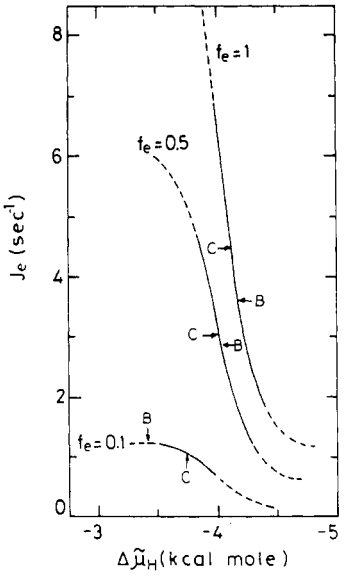

FIGURE 3: Continuous lines: rate of electron transfer, J_e, as a function of $\Delta\tilde{\mu}_H$ from state 3 to static head as would be obtained by inhibiting the ATPases, for f_e = 1, 0.5, and 0.1. The dashed lines complete the flow–force curves. Parameters of the simulations as in Figure 1. The arrows with the letters B and C mark the position of state 3 at the three values of f_e with two different sets of rate constants for the ATPase model (cases B and C; see Figures 4 and 5 and text).

Pases by the inhibition factors f_p = 0.5 or 0.1. The dashed lines show how the rate of ATP synthesis would depend on $\Delta\tilde{\mu}_H$ at $|\Delta\tilde{\mu}_H|$ higher than the state 3 values. Upon inhibition of the ATPases, state 3 is shifted to higher values of $|\Delta\tilde{\mu}_H|$ ($\Delta\tilde{\mu}_H$ = −4.0, −4.1, and −4.29 kcal/mol with f_p = 1, 0.5, and 0.1, respectively) and moves upward in the sigmoidal flow–force curve toward the saturation region. Due to the increase in $|\Delta\tilde{\mu}_H|$ the uninhibited ATPases increase their rate. When f_p = 1 the rate of ATP synthesis in state 3 is 56% of the maximum rate, while when f_p = 0.5 and 0.1 it is 69% and 85%, respectively.

Figure 3 (continuous line) shows the rate of electron transfer J_e as a function of $\Delta\tilde{\mu}_H$ varying from state 3 to static head (as would be obtained by progressively inhibiting the ATPase pumps) in the absence of redox inhibitor (f_e = 1) or in the

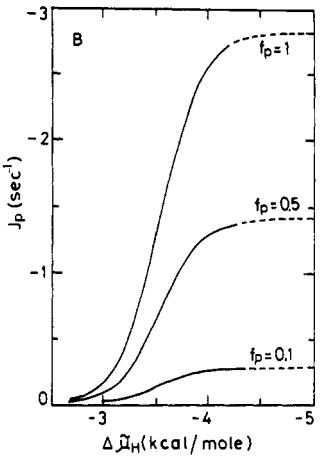

FIGURE 4: Rate of ATP synthesis as a function of $\Delta\tilde{\mu}_H$ as in Figure 2 but with different rate constants in the simulation of the ATPase pump (case B).

presence of concentrations of redox inhibitor that decrease the number of redox pumps by the inhibition factors f_e = 0.5 or 0.1. The dashed lines complete the flow–force curves. Inhibition of the redox pumps determines a shift of state 3 to lower $|\Delta\tilde{\mu}_H|$ toward the saturation region ($\Delta\tilde{\mu}_H$ = −4.0, −3.87, and −3.47 kcal/mol with f_e = 1, 0.5, and 0.1, respectively). Due to the diminished $\Delta\tilde{\mu}_H$ back-pressure the uninhibited redox pumps increase their rate. At each f_e, upon inhibition of the ATPases $|\Delta\tilde{\mu}_H|$ increases.

In the preceding paper we have shown that in the linear case in the presence of a negligible leak the flux control and the relative inhibition of J_p by an inhibitor of either the redox or the ATPase pumps are uniquely determined by the ratio $r \equiv n_p^2L_p/(n_e^2L_e)$. The quantities $n_p^2L_p$ and $n_e^2L_e$ represent the conductances of the ATPases and of the redox pumps, respectively, in the chemiosmotic protonic circuit. We have previously called them the "readinesses" with which the proton influx through the ATPases and the proton efflux through the redox pumps, respectively, change in response to a change in $\Delta\tilde{\mu}_H$. In the nonlinear case these "readinesses" are given by the tangents to the flow–force curves a and b in Figure 1, which are in general different at different values of $\Delta\tilde{\mu}_H$. With fully coupled pumps, the parameters equivalent to $n_p^2L_p$ and $n_e^2L_e$ are therefore $n_p(\partial J_p/\partial\Delta\tilde{\mu}_H)$ and $n_e(\partial J_e/\partial\Delta\tilde{\mu}_H)$, respectively. The ratio r in the nonlinear case becomes $r_{nl} \equiv n_p(\partial J_p/\partial\Delta\tilde{\mu}_H)/[n_e(\partial J_e/\partial\Delta\tilde{\mu}_H)]$, which in general, in contrast to the linear case, is different at different values of $\Delta\tilde{\mu}_H$ (cf. Figures 2 and 3). In a double-inhibitor titration with nonlinear flow–force relationships, the behavior will be different from that found with the linear model whenever the changes in $\Delta\tilde{\mu}_H$ which accompany partial inhibition of one of the pumps, at any given concentration of inhibitor of the other pump, give rise to different values of r_{nl}.

In our model the kind of change observed in r_{nl} at the $\Delta\tilde{\mu}_H$ obtaining with inhibitor, relative to that at the $\Delta\tilde{\mu}_H$ obtaining without inhibitor, depends essentially on the location of state 3 in the sigmoidal flow–force relationships. From Figure 1 it is clear that this location depends on the relative positions of the flow–force curves (a and b) of the redox and ATPase pumps, or in other words, on the range of $\Delta\tilde{\mu}_H$ that controls the influx through the ATPases with respect to that which controls the efflux through the redox pumps. Moreover, it also depends on the relative sensitivity of the two pumps to $\Delta\tilde{\mu}_H$, i.e., on r_{nl} in the regions of approximate linearity around the inflection points and on the relative number of redox and ATPase pumps. By choosing different sets of rate constants

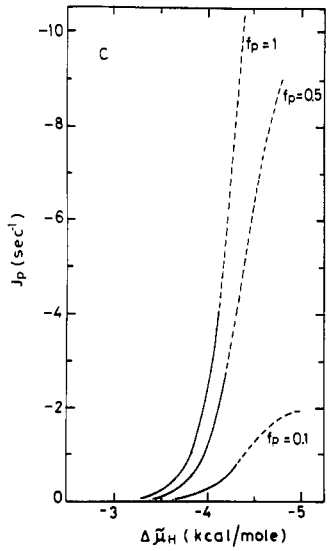

FIGURE 5: Rate of ATP synthesis as a function of $\Delta\tilde{\mu}_H$ as in Figures 2 and 4 but with different rate constants in the simulation of the ATPase pump (case C).

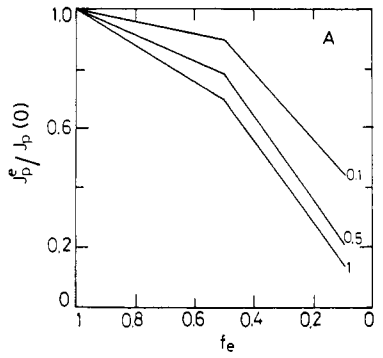

FIGURE 6: Normalized rate of ATP synthesis at different values of the inhibition factor of the redox pumps, f_e, in the absence ($f_p = 1$) and in the presence ($f_p = 0.5$ and 0.1) of an ATPase inhibitor. $J_p(0)$ is the rate of ATP synthesis at $f_e = 1$. With $f_p = 0.5$ and 0.1 $J_p(0)$ is 62% and 16%, respectively, of its value with $f_p = 1$. Parameters in the simulations as in Figures 1–3 (case A).

for the ATPase pump model, we could change the position and the slope of the flow–force curve of the ATPase pump relative to those of the redox pump and obtain case B shown in Figure 4 and case C shown in Figure 5 (to be compared with the previously discussed case A in Figure 2).

In case B (Figure 4) state 3 falls almost in the saturation region, and upon partial inhibition of the ATPases it moves further into it. The rate of ATP synthesis in state 3 ($f_p = 1$) is 97% of the maximum rate, and it becomes 98% and 99% when $f_p = 0.5$ and 0.1, respectively. In case C (Figure 5) state 3 falls below the beginning of the region of approximate linearity and upon inhibition of the ATPases it moves into it. When $f_p = 1$ the rate of ATP synthesis in state 3 is 20% of the maximum rate, while when $f_p = 0.5$ and 0.1 it becomes 26% and 40%, respectively. In Figure 3 the arrows with the letters B and C mark the position of state 3 ($f_p = 1$) for cases B and C, respectively, in the flow–force curves J_e vs. $\Delta\tilde{\mu}_H$ at the three different values of f_e.

Figures 6 and 7 show the simulated titrations with a redox inhibitor in the absence or presence of ATPase inhibitor for a chemiosmotic system with the nonlinear flow–force relationships shown in Figures 2 and 3 (case A), and 5 and 3 (case C), respectively. In case A (Figure 6) as in case B (not shown) and in the linear model, the relative inhibition of the rate of ATP synthesis by a given concentration of redox inhibitor is

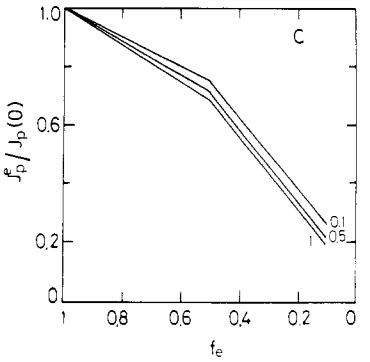

FIGURE 7: Normalized titrations with a redox inhibitor as in Figure 6, with kinetic parameters in the simulations as in Figure 5 (case C). With $f_p = 0.5$ and 0.1 $J_p(0)$ is 65% and 20%, respectively, of its value with $f_p = 1$.

lower when the ATPases are partially inhibited. In case C (Figure 7) the difference in the relative inhibition of the rate of ATP synthesis when the ATPases are either partially or not inhibited is very small and could well be below experimental detectability.

An analysis with the help of Figures 3 and 5 of the comparison between r_{nl} at the higher $|\Delta\tilde{\mu}_H|$ obtaining in the presence of ATPase inhibitor and at the lower $|\Delta\tilde{\mu}_H|$ obtaining in the absence of inhibitor, at any given f_e, explains the behavior seen in case C (Figure 7). Consider a 90% inhibition of the ATPases ($f_p = 0.1$). Figure 5 shows that state 3 goes from $\Delta\tilde{\mu}_H = -4.12$ kcal/mol to $\Delta\tilde{\mu}_H = -4.31$ kcal/mol. The value of the tangent $\partial J_p/\partial\Delta\tilde{\mu}_H$ to each curve shown in Figure 5 increases as $|\Delta\tilde{\mu}_H|$ increases. At $\Delta\tilde{\mu}_H = -4.12$ Kcal/mol (state 3 in the absence of inhibitors) the tangent to the curve with $f_p = 0.1$ is exactly one-tenth as great as the tangent to the curve with $f_p = 1$ at the same value of $\Delta\tilde{\mu}_H$. In general, at any given f_p, the value of the tangent in the presence of ATPase inhibitor is f_p times that in its absence at the same value of $\Delta\tilde{\mu}_H$

$$(\partial J_p/\partial\Delta\tilde{\mu}_H)_{f_p,\Delta\tilde{\mu}_H} = f_p(\partial J_p/\partial\Delta\tilde{\mu}_H)_{\Delta\tilde{\mu}_H}$$

However, in the presence of inhibitor, state 3 shifts to higher $|\Delta\tilde{\mu}_H|$ where the tangent is higher, and therefore, with the flow–force relationship in Figure 5, $\partial J_p/\partial\Delta\tilde{\mu}_H$ in the presence of ATPase inhibitor is higher than f_p times $\partial J_p/\partial\Delta\tilde{\mu}_H$ in its absence

$$(\partial J_p/\partial\Delta\tilde{\mu}_H)_{f_p} > f_p(\partial J_p/\partial\Delta\tilde{\mu}_H)$$

Moreover Figure 3 shows that the value of the tangent $\partial J_e/\partial\Delta\tilde{\mu}_H$ to the curves with $f_e = 1$ and 0.5 decreases slightly as $|\Delta\tilde{\mu}_H|$ increases above the state 3 value (−4.12 Kcal/mol). Therefore, at least for f_e values that are not too small, $\partial J_e/\partial\Delta\tilde{\mu}_H$ in the presence of ATPase inhibitor is slightly lower than $\partial J_e/\partial\Delta\tilde{\mu}_H$ in its absence

$$(\partial J_e/\partial\Delta\tilde{\mu}_H)_{f_p} < (\partial J_e/\partial\Delta\tilde{\mu}_H)$$

As a consequence, in contrast with the linear model in which the ratio r in the presence of ATPase inhibitor is always lowered by the factor f_p as compared with its value in the absence of inhibitor, in case C of the nonlinear model the ratio r_{nl} changes little in the presence of ATPase inhibitor. There is only a small redistribution of flux control between the redox and ATPase pumps and therefore similar titration curves are obtained.

Actually with nonlinear kinetics characterized by a very sharp increase of the rate of ATP synthesis and a decrease of the rate of electron transfer as $|\Delta\tilde{\mu}_H|$ increases, the ratio r_{nl} could be even higher in the presence of ATPase inhibitor than

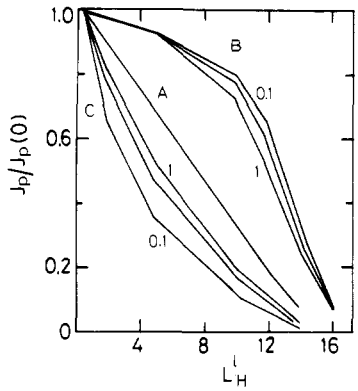

FIGURE 8: Normalized rate of ATP synthesis at different values of the leak conductance, L_H^l, in the absence ($f_p = 1$) and in the presence ($f_p = 0.5$ and 0.1) of an ATPase inhibitor, for the three different cases A, B, and C (cf. Figures 2, 4, and 5).

in its absence, thus leading to a lower flux control by the ATPases and to a result opposite to that intuitively expected in a double-inhibitor titration.

The simulations in Figures 6 and 7 were performed with a small Ohmic proton leak ($L_H^l/n_eL_e = 6 \times 10^{-3}$, where n_eL_e is the slope of the region of approximate linearity of the J_H vs. $\Delta\tilde{\mu}_H$ curve for the redox pump). An increase of the leak conductance reduces the difference in the titration curves as was seen in the linear case. A sufficiently high leak can lead to identical titration curves in both kinds of double-inhibitor experiments. If the leak is non-Ohmic and the conductance of the membrane increases sharply as $|\Delta\tilde{\mu}_H|$ increases, a high leak could even lead to higher relative inhibition of the rate of ATP synthesis by a certain concentration of redox inhibitor in the presence of ATPase inhibitor as compared with its absence. In terms of control theory this happens when, at the higher $|\Delta\tilde{\mu}_H|$ reached in the presence of ATPase inhibitor, the gain in negative flux control by the leak is higher than the gain in positive flux control by the ATPases, so that the redox pumps increase their flux control [since the sum of the flux controls equals 1 as shown by Kacser and Burns (1973)] (cf. also eq 14A in the Appendix of the preceding paper). In the other kind of double-inhibitor titration, however, a high nonlinear leak should never lead to higher relative inhibition of the rate of ATP synthesis by a certain concentration of ATPase inhibitor in the presence of redox inhibitor. In fact, at the lower $|\Delta\tilde{\mu}_H|$ obtaining in the presence of redox inhibitor the negative flux control of the leak decreases, thus allowing a higher decrease of the flux control of the ATPases in comparison with the linear model.

Simulations of uncoupler–inhibitor titrations for the three different cases of nonlinear flow–force relationships A, B, and C are shown in Figure 8. In case C, as in the linear case (see accompanying paper), the relative decrement in the rate of phosphorylation at any given L_H^l is higher in the presence of ATPase inhibitor than in its absence, while in case B the opposite is true. In case A the relative inhibition is the same with or without ATPase inhibitor. In all three cases the relative decrease in $|\Delta\tilde{\mu}_H|$ induced by a certain concentration of uncoupler is larger in the presence of ATPase inhibitor than in its absence, as in the linear case (not shown). However, in contrast to the linear case, the relative decrease in J_p is not proportional to the relative decrease in $\Delta\tilde{\mu}_H$ induced by the uncoupler (see preceding paper).

Discussion

We have shown in the preceding paper that, with linear flow–force relationships, in a delocalized chemiosmotic model of energy coupling (in the presence of a negligible leak) the relative inhibition of the rate of ATP synthesis, by a given combination of inhibitors of the redox and ATPase proton pumps, is exclusively dependent on the ratio $n_p^2L_p/(n_e^2L_e) = r$ between the conductances of the two proton pumps in the chemiosmotic protonic circuit. The distribution of flux control between the two pumps exclusively depends on the same ratio. In different conditions of inhibition (e.g., in the presence of an ATPase inhibitor at any given concentration of redox inhibitor) the ratio of the conductances is bound to change in the linear model (e.g., in the presence of an ATPase inhibitor it decreases proportionally to the fraction of inhibited ATPases). As a consequence there is a redistribution of flux control between the two pumps and a different relative inhibition of the rate of ATP synthesis in the different conditions of inhibition.

With nonlinear flow–force relations the parameter equivalent to r is $r_{nl} \equiv n_p(\partial J_p/\partial\Delta\tilde{\mu}_H)/[n_e(\partial J_e/\partial\Delta\tilde{\mu}_H)]$, which in general, in contrast to the linear case, is different at different values of $\Delta\tilde{\mu}_H$. With nonlinear relationships between the rate of ATP synthesis and/or the rate of electron transfer and $\Delta\tilde{\mu}_H$, an invariance of r_{nl} (and therefore of the distribution of flux control between the pumps and of the relative inhibition of the flow) in different conditions of inhibition is possible, provided that $(\partial J_p/\partial\Delta\tilde{\mu}_H)$ increases and/or $(\partial J_e/\partial\Delta\tilde{\mu}_H)$ decreases as $|\Delta\tilde{\mu}_H|$ increases. In fact in this case at the higher $|\Delta\tilde{\mu}_H|$ obtaining in the presence of an ATPase inhibitor $(\partial J_p/\partial\Delta\tilde{\mu}_H)$ could be sufficiently higher and/or $(\partial J_e/\partial\Delta\tilde{\mu}_H)$ sufficiently lower, with respect to their values at the $\Delta\tilde{\mu}_H$ obtaining without inhibitor, to counteract the inherent decrease in $(\partial J_p/\partial\Delta\tilde{\mu}_H)/(\partial J_e/\partial\Delta\tilde{\mu}_H)$ that would follow partial inhibition of the ATPases in the linear case. If at the higher $\Delta\tilde{\mu}_H$ obtaining with ATPase inhibitor $(\partial J_p/\partial\Delta\tilde{\mu}_H)$ is sufficiently higher and $(\partial J_e/\partial\Delta\tilde{\mu}_H)$ is sufficiently lower than their values at the $\Delta\tilde{\mu}_H$ obtaining without inhibitor, it is also possible that the ratio r_{nl} may increase (instead of decreasing) in the presence of ATPase inhibitor. This has the consequence that the relative inhibition by a given concentration of redox inhibitor may increase upon partial inhibition of the ATPases (cf. Stoner, 1985).

The same kinetic characteristics could lead to analogous behavior in the other kind of double-inhibitor titration, since at the lower $|\Delta\tilde{\mu}_H|$ obtaining in the presence of redox inhibitor $(\partial J_p/\partial\Delta\tilde{\mu}_H)$ could be sufficiently lower and/or $(\partial J_e/\partial\Delta\tilde{\mu}_H)$ sufficiently higher, with respect to their values at the $\Delta\tilde{\mu}_H$ obtaining without inhibitor, to counteract the inherent increase in $(\partial J_p/\partial\Delta\tilde{\mu}_H)/(\partial J_e/\partial\Delta\tilde{\mu}_H)$ that would follow partial inhibition of the redox pumps in the linear case. In our modeling study only the flow–force relationships for case C (see Figures 3 and 5) have kinetic characteristics similar to those required to obtain identical titration curves under different inhibition conditions. The kinetics used by Davenport (1985) in his simple nonlinear model of delocalized chemiosmotic coupling in chloroplasts to simulate double-inhibitor experiments evidently met these characteristics. This, and not the arguments independent of the kinetics of the flow–force relationships developed by the author, explains why he obtained equal normalized titration curves with a redox inhibitor with and without ATPase inhibitor.

The same kinetic properties (increase of $(\partial J_p/\partial\Delta\tilde{\mu}_H)$ and/or decrease of $(\partial J_e/\partial\Delta\tilde{\mu}_H)$ as $|\Delta\tilde{\mu}_H|$ increases) that can give rise to identical normalized titration curves in a double-inhibitor experiment give rise in an uncoupler–inhibitor titration, at any given concentration of uncoupler, to a larger relative decrease of the rate of ATP synthesis in the presence of an ATPase

inhibitor than in its absence (see Figure 8, case C).

In summary, with nonlinear flow–force relationships such that as $|\Delta\tilde{\mu}_H|$ increases $(\partial J_p/\partial\Delta\tilde{\mu}_H)$ increases and/or $(\partial J_e/\partial\Delta\tilde{\mu}_H)$ decreases, the experimental results of double-inhibitor and uncoupler–inhibitor titrations that have been considered in conflict with delocalized schemes of energy coupling (Baum et al., 1971; Hitchens & Kell, 1982, 1983; Venturoli & Melandri, 1982; Westerhoff et al., 1983; Berden et al., 1984) can be simulated within a delocalized chemiosmotic model. A primary conclusion of this study is therefore that the double-inhibitor and uncoupler–inhibitor approaches by themselves cannot unequivocally discriminate between "delocalized" and "localized" chemiosmotic mechanisms. It is necessary to look at the relationships between rate of ATP synthesis and $\Delta\tilde{\mu}_H$ and between rate of electron transfer and $\Delta\tilde{\mu}_H$.

The crucial question becomes do the measured flow–force relationships have the kinetic properties required to account for an invariant (or even higher) effectiveness of an inhibitor of, say, the redox pumps in the presence of an ATPase inhibitor (and vice versa)? The relationship between rate of ATP synthesis and $\Delta\tilde{\mu}_H$ obtained by inhibiting the electron transfer in mitochondria (e.g., Zoratti et al., 1982; Mandolino et al., 1983; Yagi et al., 1984) or by varying the light intensity in photophosphorylating systems (e.g., Graber & Witt, 1976; Baccarini Melandri et al., 1977; Hangarter & Good, 1982; Clark et al., 1983) and that between rate of electron transfer and $\Delta\tilde{\mu}_H$ obtained by inhibiting the ATPases in mitochondria (Zoratti et al., 1982: data from Figure 1 conveniently replotted) do show an increase in $(\partial J_p/\partial\Delta\tilde{\mu}_H)$ and a decrease in $(\partial J_e/\partial\Delta\tilde{\mu}_H)$ as $|\Delta\tilde{\mu}_H|$ increases. However, in screening the literature for the published flow–force relationships one immediately faces the problem that by varying $\Delta\tilde{\mu}_H$ with either uncouplers or ionophores different flow–force relationships not showing the required kinetic properties have been found (Padan & Rottenberg, 1973; Baccarini Melandri et al., 1977; Azzone et al., 1978a; Wilson & Forman, 1982; Zoratti et al., 1982; Mandolino et al., 1983). Different flow–force relationships depending on how $\Delta\tilde{\mu}_H$ is varied are not expected with a delocalized chemiosmotic model unless the different ways of varying $\Delta\tilde{\mu}_H$ affect the kinetics of the ATPase pump differently (when the relationship between rate of ATP synthesis and $\Delta\tilde{\mu}_H$ is considered) or the kinetics of the redox pump differently (when the relationship between rate of electron transfer and $\Delta\tilde{\mu}_H$ is considered). A possibility that would lead to a consistent picture within a chemiosmotic model that can still be regarded as delocalized since $\Delta\tilde{\mu}_H$ remains the thermodynamically competent driving force for ATP synthesis is the regulation of the kinetics of both pumps by a localized interaction (Skulachev, 1982) between them. Another possibility that has been discussed (Westerhoff et al., 1984) and in the case of chloroplasts demonstrated (Mills & Mitchell, 1984; Graber et al., 1984; Rumberg & Beecher, 1984) is the regulation of the number of active ATPases by the redox state of one or more components of the electron-transfer chain. In both cases the appropriate flow–force relationships to consider in analyzing the results of double-inhibitor experiments would be those obtained with inhibitors, and therefore it is not excluded that these results could be accommodated within a delocalized chemiosmotic model. However, the picture remains consistent only as long as results of steady-state kinetic measurements are considered. The thermodynamic inconsistencies between input force ($\Delta\tilde{\mu}_H$) and output force (affinity of the ATP hydrolysis reaction) (Wiechmann et al., 1975; Azzone et al. 1978b; Westerhoff et al., 1981; Wilson & Forman, 1982) recently accurately confirmed [Petronilli et al. (1986) in contrast to Woelders et al. (1985)] cannot be accounted for by local regulation of the kinetics.

ACKNOWLEDGMENTS

We thank Prof. G. F. Azzone for his constant support and for stimulating discussions.

Registry No. ATP, 56-65-5; H^+, 12408-02-5.

REFERENCES

Azzone, G. F., Pozzan, T., Massari, S., Bragadin, M., & Pregnolato, L. (1978a) *Biochim. Biophys. Acta 501*, 296–306.

Azzone, G. F., Pozzan, T., & Massari, S. (1978b) *Biochim. Biophys. Acta 501*, 307–316.

Baccarini Melandri, A., Casadio, R., & Melandri, B. A. (1977) *Eur. J. Biochem. 78*, 389–402.

Baum, H., Hall, G. S., Nalder, J., & Beechey, R. (1971) in *Energy Transduction in Respiration and Photosynthesis* (Quagliariello, E., et al., Eds.) pp 747–755, Adriatica Editrice, Bari.

Berden, J. A., Herweijer, M. A., & Cornelissen, J. B. W. T. (1984) in *H^+-ATPase (ATP Synthase) Structure, Function, Biogenesis. The F_0–F_1 Complex of Coupling Membranes* (Papa, S., et al., Eds.) pp 339–348, ICSU Press and Adriatica Editrice, Bari.

Chapman, J. B., Johnson, E. A., & Kootsey, J. M. (1983) *J. Membr. Biol. 74*, 139–153.

Clark, A. J., Cotton, N. P. J., & Jackson, T. B. (1983) *Biochim. Biophys. Acta 723*, 440–453.

Davenport, J. W. (1985) *Biochim. Biophys. Acta 807*, 300–307.

Gräber, P. (1982) *Curr. Top. Membr. Transp. 16*, 215–245.

Gräber, P., & Witt, H. T. (1976) *Biochim. Biophys. Acta 423*, 141–163.

Gräber, P., Schlodder, E., & Witt, H. T. (1984) in *H^+-ATPase (ATP Synthase) Structure, Function, Biogenesis. The F_0–F_1 Complex of Coupling Membranes* (Papa, S., et al., Eds.) pp 431–440, Adriatica Editrice, Bari.

Hangarter, R. P., & Good, N. E. (1982) *Biochim. Biophys. Acta 681*, 397–404.

Hansen, U. P., Gradmann, D., Sanders, A., & Slayman, C. L. (1981) *J. Membr. Biol. 63*, 165–190.

Hitchens, G. D., & Kell, D. B. (1982) *Biochem. J. 206*, 351–357.

Hitchens, G. D., & Kell, D. B. (1983) *Biochim. Biophys. Acta 723*, 308–316.

Kacser, H., & Burns, J. A. (1973) in *Rate Control of Biological Processes* (Davis, D. D., Ed.) pp 65–104, Cambridge University Press, Cambridge, U.K.

Läuger, P. (1984) *Biochim. Biophys. Acta 779*, 307–341.

Maloney, P. C., & Hansen, F. C., III (1982) *J. Membr. Biol. 66*, 63–75.

Mandolino, G., De Santis, A., & Melandri, B. A. (1983) *Biochim. Biophys. Acta 723*, 428–439.

Mills, J. D., & Mitchell, P. (1984) *Biochim. Biophys. Acta 764*, 93–104.

Mitchell, P. (1966) *Chemiosmotic Coupling in Oxidative and Photosynthetic Phosphorylation*, Glynn Research Ltd., Bodmin, U.K.

Nicholls, D. G. (1974) *Eur. J. Biochem. 49*, 573–583.

Padan, E., & Rottenberg, H. (1973) *Eur. J. Biochem. 40*, 431–437.

Petronilli, V., Pietrobon, D., Zoratti, M., & Azzone, G. F. (1986) *Eur. J. Biochem. 155*, 423–431.

Pietrobon, D., & Caplan, S. R. (1985) *Biochemistry 24*, 5764–5776.

Pietrobon, D., Azzone, G. F., & Walz, D. (1981) *Eur. J. Biochem. 117*, 389-394.
Pietrobon, D., Zoratti, M., Azzone, G. F., Stucki, J. W., & Walz, D. (1982) *Eur. J. Biochem. 127*, 483-494.
Pietrobon, D., Zoratti, M., Azzone, G. F., & Caplan, S. R. (1986) *Biochemistry 25*, 767-775.
Rumberg, B., & Becher, U. (1984) in *H^+-ATPase (ATP Synthase) Structure, Function, Biogenesis. The F_0-F_1 Complex of Coupling Membranes* (Papa, S., et al., Eds.) pp 421-430, Adriatica Editrice, Bari.
Skulachev, V. P. (1982) *FEBS Lett. 146*, 1-4.
Stoner, C. D. (1985) *J. Bioenerg. Biomembr. 17*, 85-108.
van Dam, K., Westerhoff, H. V., Krab, K., van der Meer, R., & Arents, J. C. (1980) *Biochim. Biophys. Acta 591*, 240-250.
Venturoli, G., & Melandri, B. A. (1982) *Biochim. Biophys. Acta 680*, 8-16.
Westerhoff, H. V. (1983) Ph.D. Thesis, University of Amsterdam, Amsterdam, The Netherlands.
Westerhoff, H. V., Simonetti, A. L. M., & van Dam, K. (1981) *Biochem. J. 200*, 193-202.
Westerhoff, H. V., Colen, A. M., & van Dam, K. (1983) *Biochem. Soc. Trans. 11*, 81-85.
Westerhoff, H. V., Melandri, B. A., Venturoli, G., Azzone, G. F., & Kell, D. B. (1984) *Biochim. Biophys. Acta 768*, 257-292.
Wiechmann, A. H. C. A., Beem, E. P., & van Dam, K. (1975) in *Electron Transfer Chains and Oxidative Phosphorylation* (Quagliariello, E., et al., Eds.) pp 335-342, North-Holland, Amsterdam.
Wilson, D. F., & Forman, N. G. (1982) *Biochemistry 21*, 1438-1444.
Woelders, H., van der Zande, W. J., Colen, A. M. A. F., Wanders, R. J. A., & van Dam, K. (1985) *FEBS Lett. 179*, 278-282.
Yagi, T., Matsuno-Yagi, A., Vik, S. B., & Hatefi, Y. (1984) *Biochemistry 23*, 1029-1036.
Zoratti, M., Pietrobon, D., & Azzone, G. F. (1982) *Eur. J. Biochem. 126*, 443-451.
Zoratti, M., Petronilli, V., & Azzone, G. F. (1986) *Biochim. Biophys. Acta 851*, 123-135.

Production of Interleukin 1 by SK Hepatoma Tumor Cells

William M. Moore, William N. Wester, and Curtis A. Spilburg*,‡
Searle Research and Development, c/o Monsanto Company, St. Louis, Missouri 63198
Received June 12, 1986; Revised Manuscript Received August 7, 1986

ABSTRACT: SK hepatoma cells and SK hepatoma conditioned media contain an 18 000-dalton factor which is pyrogenic, stimulates collagenase and prostaglandin production in skin and synovial fibroblasts, induces bone resorption, and stimulates the proliferation of murine thymocytes. These results are consistent with the finding that this tumor cell line produces interleukin 1 [Doyle, M. V., Brindley, L., Kawasaki, E., & Larrick, J. (1985) *Biochem. Biophys. Res. Commun. 130*, 768-773] since all these activities have been associated with this cytokine. Greater than 80% of the cellular activity has a molecular weight of 30 000, while in contrast, greater than 80% of the activity in the tumor-conditioned media has a molecular weight of 18 000. When active material from the cells is incubated with trypsin, this high molecular weight material is completely converted into an active 18 000 molecular weight species. The isoelectric point of all active material is always between p*I* 4.0 and 5.1, regardless of molecular weight. All of these results are consistent with the hypothesis that active, high molecular weight interleukin 1α is first synthesized and stored by the tumor cell. This cytokine is then cleaved by a trypsin-like protease to an active, lower molecular weight species which can be secreted into the media.

Interleukin 1 (IL-1)[1] is a small polypeptide hormone produced by activated macrophages (Gery et al., 1972). While it was first identified by its ability to stimulate thymocyte proliferation via induction of interleukin 2 release, it is now known to possess a much wider array of activities. Recently, cDNA clones for two distinct IL-1 species, IL-1α and IL-1β, were isolated from lipopolysaccharide-stimulated macrophage RNA, and the corresponding amino acid sequences of both forms were determined (March et al., 1985). From these studies, it was shown that both forms of the cytokine are first synthesized by the cell as 30 000-dalton precursors, which then undergo proteolytic cleavage to an 18 000-dalton form.

Many pathogenic molecules which were previously thought to be unique species are now believed to be some form of IL-1. For example, in rheumatoid arthritis, mononuclear cells have been shown to produce mononuclear cell factor (MCF) which induces the synovial cells lining the joint capsule to produce collagenase, the enzyme responsible for the irreversible destruction of the joint (Dayer et al., 1977a,b, 1980). Recently, it was shown that IL-1 has the same biological activities as those found in MCF (Mizel et al., 1981). Conversely, when MCF is added to thymocytes, uptake of tritiated thymidine is stimulated, an activitiy characteristic of IL-1. In addition, the molecular weights, isoelectric points, and sensitivity to

* Correspondence should be addressed to this author.
‡ Present address: Cardiovascular Division, Jewish Hospital, Washington University School of Medicine, St. Louis, MO 63110.

[1] Abbreviations: IL-1, interleukin 1; DMEM, Dulbecco's modified Eagle's medium; PBS, phosphate-buffered saline; FBS, fetal bovine serum; PGE_2, prostaglandin E_2; SDS, sodium dodecyl sulfate; LAF, lymphocyte activating factor; MCF, mononuclear cell factor; EDTA, ethylenediaminetetraacetic acid; Bis-Tris, 2-[bis(2-hydroxyethyl)amino]-2-(hydroxymethyl)-1,3-propanediol; Tris-HCl, tris(hydroxymethyl)-aminomethane hydrochloride.

0006-2960/86/0425-7696$01.50/0